P50
13:00 – 14:30

A Rigorous Vectorial Gaussian Beam Modeling of Virtually-Imaged-Phased-Array

A. Mokhtari, A. A. Shishegar
Department of Electrical Engineering, Sharif University of Technology, Tehran, Iran
amokhtari@ee.sharif.edu,shishegar@sharif.edu

Abstract *The Virtually-Imaged-Phased-Array (VIPA) is a modified version of etalon used as a hyperfine spectral disperser. We have developed an analytical Gaussian beam tracing formulation which can model the VIPA output pattern and the effects of polarization changes*.

Introduction

Spectral dispersers play a key role in optical signal processing by spatially separating the optical frequencies. They have a wide variety of applications such as wavelength demultiplexing, dispersion compensation, femtosecond pulse shaping. Well-known spectral dispersers like prism and diffraction grating do not provide sufficient resolution required for thin channel spacing of dense wavelength multiplexing [1, 2, 3]. To overcome this problem, new spectral dispersers like Arrayed Waveguide Grating (AWG) and VIPA have been proposed. Shiarasaki [1] demonstrated that the VIPA-based multiplexer /demultiplexer has better performance, simple and compact design, and polarization insensitivity. He also introduced the VIPA with graded reflectivity to improve the performance later [2]. Novel applications of VIPA in optical pulse shaping such as OCDMA encoder/decoder [3], photonic-microwave arbitrary waveform generation [4], and programmable optical burst manipulation [5] have also been reported in the literature.

The VIPA principal system is depicted in fig1. The VIPA operation can be explained based on the Fabry-Perót etalon. It consists of two high reflective coated plates. The input (entry) side has a reflectivity factor close to 1. A window remains uncoated or coated with anti-reflection (AR) material to allow light beam entrance. There are two types of VIPA depending on the dielectric material that the etalon cavity is filled with. If the VIPA medium between two plates is air, it is called air-filled VIPA; otherwise it is called solid VIPA.

The laser source beam is focused on the output plate of the etalon. The collimated beam enters the etalon through the anti reflection (AR) coated window and reflects back and forth. During each reflection from output side, a portion of the light power emits out of the VIPA. The reflection continues until all injected power leaks out of the VIPA. The VIPA operation can be viewed best as the interference of an infinite number of waves from virtual sources (VS) of progressively smaller amplitudes and equal phase differences [6].

The multiple diverging beams from virtual sources interfere with each other and form a collimated beam. The phase differences between the diverging beams are highly sensitive to the wavelength variations. As wavelength changes, the collimated beam's output angle varies and results in hyperfine angular dispersion.

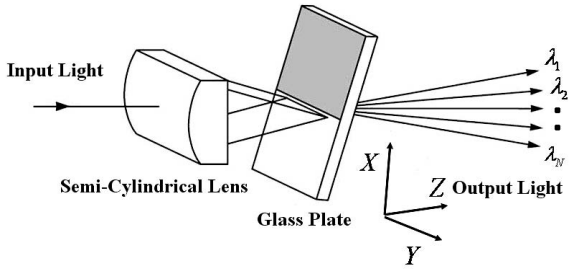

Fig1: VIPA as a spectral disperser [2]

There are a few analytical treatments in the literature suffering from restricting assumptions. Long Yang [7] modeled VIPA with 1-D Gaussian beam as a periodic filter and calculated the maxima of pass bands as a function of diffraction angle. Vega et al [8] proposed a grating equation based on a plane wave theory for relatively large incident angles. Xiao et al [9] took into account the paraxial waves and generalized the Vega approach to the small incident angles.

Vectorial Gaussian beam derivation

Consider the problem of three homogeneous lossless media n_1, n_2 and n_3 separated by two parallel planes as illustrated in fig2. A laser output beam considered as an elliptic vectorial Gaussian beam (1) passes distance Z_0 to intercept the output plane. This interception results in two new beams: reflected (2) and transmitted (3) and the same process will go on.
Incident elliptic Gaussian beam in the primed (beam-based) coordinate (x'_1, y'_1, z'_1) with origin at P_1 on the source is [10]: $k_1 = \omega\sqrt{\varepsilon_1\mu_1}$

$$\underline{E}^i(x'_1, y'_1, z'_1) = \begin{pmatrix} E_{0x'_1} \\ E_{0y'_1} \end{pmatrix} \frac{1}{\sqrt{W_{x'_1}(z'_1) W_{y'_1}(z'_1)}} \quad (1)$$

$$\exp\{-jk_1 z'_1 - j\eta_1(z'_1) - \frac{jk_1}{2}\left(\frac{x'^2_1}{q_{x'_1}(z'_1)} + \frac{y'^2_1}{q_{y'_1}(z'_1)}\right)\}$$

Where $W_i(z'_1)$, $E_{0,i}$ and $q_i(z'_1)$ are the Gaussian beam radius, electric field's phasor and q at z'_1 on the related polarization respectively $i = (x'_1, y'_1)$.

$\eta_1(z'_1)$ is the Gaussian beam phase correction factor. The primed coordinate system changes to the incident point local coordinate system (x_1, y_1, z_1) at P_0 by a rotation α_1 (denoted by $Rot(\alpha_1)$) and a shifting Z_0. The reflected beam in its beam-based coordinate system is: $k_2 = \omega\sqrt{\varepsilon_2\mu_2}$

$$\underline{E}^r(x'_2, y'_2, z'_2) = \begin{pmatrix} E_{0x'_2} \\ E_{0y'_2} \end{pmatrix} \frac{1}{\sqrt{W_{x'_2}(z'_1) W_{y'_2}(z'_1)}} \quad (2)$$

$$\exp\{-jk_1 z'_1 - j\eta_2(z'_2) - \frac{jk_1}{2}(\frac{x'^2_2}{q_{x'_2}(z'_2)} + \frac{y'^2_2}{q_{y'_2}(z'_2)})\}$$

We follow a rigorous vectorial Gaussian beam tracing method used in [11]. There are a few unknown parameters in the reflected and transmitted beams that should be extracted from the incident known parameters through satisfying boundary conditions at the incident point. Reflected beam in its local coordinate system (x_2, y_2, z_2) is [11]:

$$\underline{E}^r(x_2, y_2, z_2) = Rot(\alpha_2) \begin{pmatrix} E_{0x'_2} \\ E_{0y'_2} \end{pmatrix} \frac{1}{\sqrt{W_{x_2}(z'_1) W_{y_2}(z'_1)}}$$

$$\exp\{-jk_1 z_2 - j\eta_2(z_2) - \frac{jk_1}{2} \begin{pmatrix} x_2 \\ y_2 \end{pmatrix}^t \underline{\underline{Q}}^r \begin{pmatrix} x_2 \\ y_2 \end{pmatrix}\} \quad (3)$$

$$\underline{\underline{Q}}^r = Rot(\alpha_2) \begin{pmatrix} \frac{1}{q_{x_2}(z_2)} & 0 \\ 0 & \frac{1}{q_{y_2}(z_2)} \end{pmatrix} Rot(-\alpha_2)$$

The similar expression is valid for the transmitted beam (3) by changing $r \quad t, 1 \quad 2, 2 \quad 3$.

Reflected beam calculations

After a lengthy mathematical calculation, the matrix of reflected beam becomes:

$$\underline{\underline{Q}}^r = \begin{pmatrix} A & B \\ B & C \end{pmatrix} \quad (4)$$

$$A = \frac{\cos^2(\alpha_1)}{q_{x_1}(Z_0)} + \frac{\sin^2(\alpha_1)}{q_{y_1}(Z_0)}$$

$$B = \frac{\sin(2\alpha_1)}{2}(\frac{-1}{q_{x_1}(Z_0)} + \frac{1}{q_{y_1}(Z_0)})$$

$$C = \frac{\sin^2(\alpha_1)}{q_{x_1}(Z_0)} + \frac{\cos^2(\alpha_1)}{q_{y_1}(Z_0)}$$

The next step is to find the eigenvalues and eigenvectors of this matrix to derive the q-parameters and rotation angle of the reflected beam:

$$\begin{cases} q_{x_2}(0) = q_{x_1}(Z_0) \\ q_{y_2}(0) = q_{y_1}(Z_0) \end{cases}, \ \alpha_2 = -\alpha_1 \quad (5)$$

Transmitted beam calculations

Following the same approach we used for reflected beam, the transmitted beam matrix $\underline{\underline{Q}}^t$ becomes:

$$\underline{\underline{Q}}^t = \frac{k_1}{k_2} \begin{pmatrix} b^2 A & bB \\ bB & C \end{pmatrix}, \ b = \frac{\cos(\theta_i)}{\cos(\theta_o)} \quad (6)$$

$q_{x_3}(0)$ and $q_{y_3}(0)$ are complicated functions of both polarizations' q-parameters of incident beam i.e. $q_{x_1}(Z_0)$ and $q_{y_1}(Z_0)$. Other unknowns can be extracted from the Gaussian beam's q-parameters.

Following the same approach, the q-parameters for the N*th* virtual source are derived. Then all unknown electric field phasors are extractable in terms of geometrical and incident Gaussian beam parameters for the N*th* virtual source:

$$\begin{pmatrix} E_{0x'_{3N}} \\ E_{0y'_{3N}} \end{pmatrix} = Rot(-\alpha_3) \begin{pmatrix} \frac{k_1}{k_2} T_m & 0 \\ 0 & T_e \end{pmatrix} Rot(\alpha_1) \quad (7)$$

$$(Rot(-\alpha_2) \begin{pmatrix} R_m & 0 \\ 0 & R_e \end{pmatrix} Rot(\alpha_1))^{2(N-1)} \begin{pmatrix} E_{0x'_1} \\ E_{0y'_1} \end{pmatrix}$$

$$\exp\{-j(k_1 Z_0 - 2(N-1)k_1 l\}$$

Amplitude and Phase correction factors

Where (R_e, T_e) and (R_m, T_m) are the reflection and transmission amplitude coefficients for transverse electric field in TE and TM polarizations respectively.

Simulation method

Electric field's phasors at the VIPA output side are calculated Using equation (7) in its local coordinate system, and then we compute each virtual source's field on arbitrary vertical plane concerning the propagation effects on Gaussian beam parameters. Total field is obtained by shifting the local coordinate systems related to the main coordinate system and summation over all the resulted fields.

This Process yields an analytical closed form formula that is used to compute output VIPA pattern for the arbitrary scheme parameters.

This formulation is simulated for both uniform and graded Solid VIPA using reference [2] scheme based on the derived analytical relations.

Numerical results

We have used $\lambda = 1550\,nm, n_1 = n_3 = 1, n_2 = 1.5$

$\theta_i = 4.3^\circ, W_{x'_1}(0) = W_{y'_1}(0) = 5.7\,\mu m, Z_0 = 50\mu\,m,$

VIPA Thickness $= 100\,\mu m, \alpha_1 = 0^\circ \varphi = 87.5^\circ$

The number of virtual sources is 100. Suppose $R_e = R_m = \sqrt{.95} = 0.9747$ for uniform VIPA and

$R_e = R_m = \sqrt{1-(0.5X)^2}$ for graded VIPA where X is between 0 and 2mm. Fig3 shows the comparison between the results in [2] and current work. As it is depicted, fig3 (a) and (b) are the output beams with uniform and graded reflectivity respectively. Two works have a great similarity. We consider a 3-D model and took into account more details so that the model differences are irresistible**.** The method overview is as follows: 1) The Source beam waists are finite in both polarizations that are modeled as a generalized elliptic vectorial Gaussian beam.2) 3D analysis in the transverse plane 3) Precise modeling of the coating films by reflection and transmission coefficients. 4) Compatibility to treat both types of VIPA

Conclusion

We proposed a rigorous vectorial Gaussian beam formulation to derive a 3-D general model for the VIPA. The advantages and potentials of this method are also investigated**.**

Acknowledgement: This work is supported by the Iran Telecommunication Research Center (**ITRC**). Their support is appreciated.

References

1. M. Shirasaki, *Opt. Lett.*, vol. 21 (1996), pp.366–368
2. M. Shirasaki et al. *IEEE Photon. Technol. Lett.*, vol. 11 (1999), pp. 1443–1445
3. S. Etemad, et al. *OFC 2004*, FG5, 2004.
4. S. Xiao et al, *IEEE Photon. Technol. Lett.*, vol. 16 (2004), no. 8
5. G. Lee et al., *IEEE JLT*, vol. 23 (2005), no. 11
6. *E.* A. Bahaa Saleh, C. T. Malvin, "*Fundamentals of Photonics",* pp 70-72, 1991 John Wiley & Sons
7. Long Yang, *OFC 2002,* 320-321
8. A. Vega et al., *Appl. Opt.*, vol. 42 (2003), no. 20,
9. S. Xiao et al., *IEEE JQE*, vol. 40 (2004), no. 4
10. A. Rohani et al, *Optics Communications*, vol. 232 (2004), pp 1-10
11. M. Akhavan-Bahabadi et al, AP-S International Symposium (*Digest*), vol. 3 (2002), pp 332-335

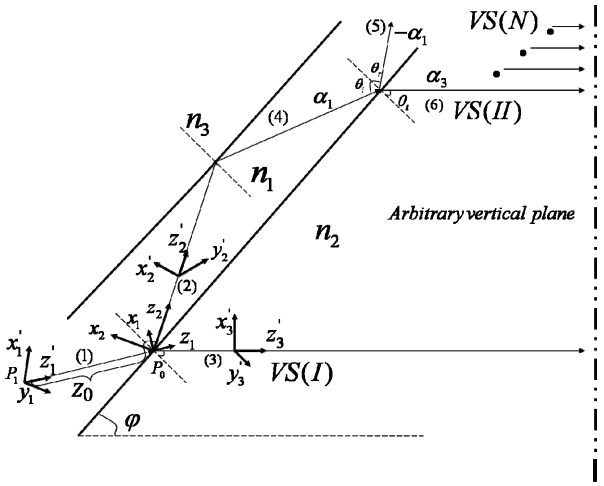

Fig2: The VIPA equivalent problem

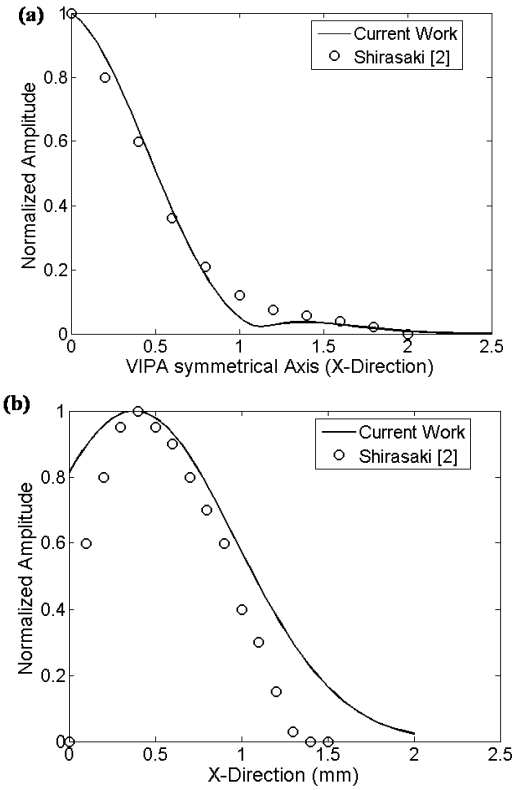

Fig3: Simulated output 2-D pattern of VIPA on the symmetrical axis of VIPA
(a) uniform with Circular Gaussian Beam (GB)
(b) Graded with Circular GB

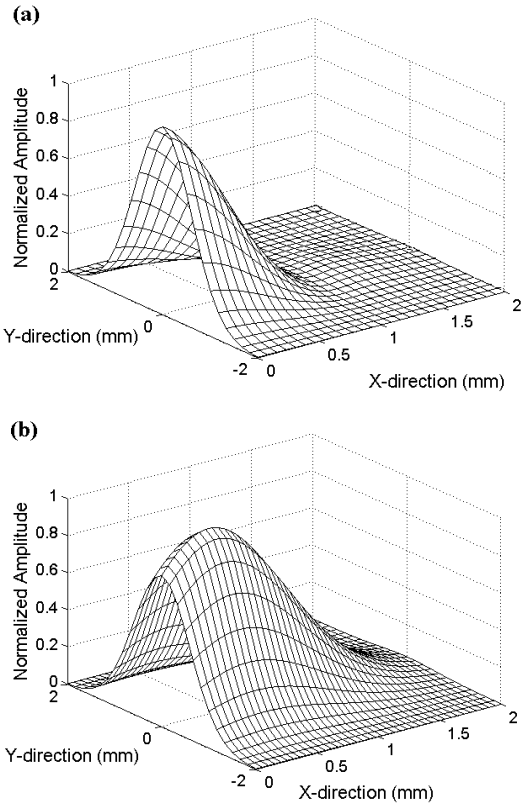

Fig4: Simulated output 3-D pattern of VIPA
(a) uniform with Circular Gaussian Beam (GB)
(b) Graded with Circular GB